Turk J Phy
24 (2000) , 567 – 576.

The Effect of Potassium Doping on Resistive Transitions and Transport Critical Current of Bulk YBCO high-T_c Superconductors

S. ÇELEBİ, A. ÖZTÜRK, I. KARACA, U. KÖLEMEN
Department of Physics, Faculty of Science and Arts,
Karadeniz Technical University,
61080 Trabzon-TURKEY
e-mail: celebi@ktu.edu.tr

Received 1999

Abstract

We report on observations of the effect of potassium in YBCO (123) high temperature superconductors with nominal composition $Y_{1-0,2x}$ $Ba_{2-0.2x}$ K_x Cu_3 O_y. The electrical resistivity measurements show that the critical temperature T_c (R=0) shifted slightly to lower temparature due to the K doping process. This process also decreases the transport critical current density and the activation energy for thermally activated flux flow. The magnetic field dependence of j_c was measured at 77 K after zero field cooling (ZFC) when the applied magnetic field is impressed (ZFCV) and removed (ZFCD). The results are discussed in terms of "return" magnetic flux density associated with the magnetization of the grains. Activation energy was determined from the Arrhenius resistivity plot versus temperature curve. The XRD patterns are also presented for sample characterization.

Key Words: High-T_c superconductors, K-doping, critical current density, resistive transition

1. Introduction

The influence of dopants on the superconducting properties of YBCO has received a great deal of attention in order to improve their partinent parameters. To our knowledge, only a few papers were published on the alkali metals impurities in the YBCO system [1-6]. Saito et al. [1] investigated the substitution effect of K for Ba in the compound $Y(Ba_{1-x}K_x)_2Cu_3O_y$ and their results show that the transition temperature, $T_c(R = 0)$ and $T_{c,midpoint}$, decreases gradually with increasing x. Khan [2] reported a

$T_{c,onset} \simeq 135$ K in a K-substituted YBCO compound. Dragieva et al. [4] studied the $Y_{1-0.2x}Ba_{2-02x}M_xCu_3O_y$ system, where $x = 0.7$, and M=Li, Na, K, and found that the transition temperature relatively increased in K-doped YBCO. Veneva et al. [6] reported on AC susceptibility studies on K-doped YBCO high-T_c superconductors wtih nominal composition $Y_{1-0.2x}Ba_{2-02x}K_xCu_3O_y$ ($x = 0 - 1.2$) where the sample with $x = 0.4$ exhibited the trongest intergranular connectivity and $T_{c,onset}$ changed only slightly with increasing x. Nedkov et al. [5] studied the influnce of alkali metal impurities on the electrical and magnetic properties of YBCO with general batch formula $Y_{1-0.2x}Ba_{2-02x}(Me_x)Cu_{3+0.3x}O_y$ (where M_e denotes Na, K, Rb). Only Rb doping of YBCO echanced the critical current density while the other dopants (Na, K) decreased it (see Table 1 of Ref. [5]).

Consequently it is desirable to provide additional observations which may shed light these conflicting results. In this work we focused on samples with the batch formula $Y_{1-0.2x}Ba_{2-02x}K_xCu_3O_y$ (where $x = 0, 0.4$) to study various aspects and also compare with the K-doped samples in the literature, particularly those of Ref. [6]. Our observations reveal that the transport critical current density decreases, as x increases in contrast with the results reported in Ref. [6], and the transition temperature (zero resistance) decreases with K doping of YBCO, which we will denote K-YBCO for brevity. We extracted activation energy from the Arrhenius plot. The hysteretic behaviors of j_c at 77 K in an externally applied field are also presented upon excursion to 6 mT.

2. Experimental

We fabricated samples with the nominal compositions $Y_{1-0.2x}Ba_{2-02x}K_xCu_3O_y$ ($x =$ 0 and 0.4) using the conventional solid state reaction in air. The powders of Y_2O_3, $BaCO_3$, CuO, K_2CO_3 were thoroughly mixed in the appropriate amounts by a grinding machine for 6 h. After milling, the mixed powders were heated at 900 °C for 24 hours. The reacted materials were reground finely and pressed into pellets of 13 mm diameter at 375 MPa. The pellets were sintered at 950 °C for 32 hours as were the samples in ref. [6]. However, partial melting was observed. Hence the same sintering treatment was repeated on the identical pellets where the sintering temperature was 935, 932, 925, 910, 890 ° for 32 hours leading to the optimum sintering temperature as 925 °C. Finallly, the pellets sintered at 925 °C for 32 hours were annealed at 550 °C for 6 hours and then cooled to room temperature at 1 °C/min. The heat treatment processes were performed in alumina crucibles.

The X-ray diffraction data were taken using a Rigaku D/Max-IIIC diffractometer with CuK_α X-ray at 40kV and 30mA with a step of 0.02^0 over the range $2\theta = 5 - 60^0$ and a scanning rate of 0.05 sec^{-1}. The measurements of the superconducting transition temperature and transport critical current of the samples were carried out by a four-probe method. Rectangular bar-shaped samples of length l, width w and thickness t of $11.42 \times 3.15 \times 1.35$ and $12.01 \times 2.75 \times 1.46$ mm^3 were cut from pellets of YBCO and K-YBCO, respectively. Current and voltage contacts on the sample were made by silver paste. We performed the resistivity measurements using a closed cycle crystat

at low temperatures down to 30 K. The magnetic field was measured by a commercial fluxmeter.

The measurements of the critical transport currents as a function of magnetic field were performed with immersed in an open liquid nitrogen bath at 77 K. The critical current I_c is defined by the electric field 1μV/mm (criterion voltage was 5 μV). Hence the sample was placed at the center of Helmholtz coils providing the magnetic field. The current in the sample was directed perpendicular to the applied field directed along thickness (i.e. along the axis of compression).

In the measurements of the j_c dependence on magnetic field, two procedures were followed, namely, zero field cooling (ZFC) and field cooling (FC). In the ZFC procedure, the sample is allowed to cool from above T_c to the 77 K ambient temperature in the absence of a magnetic field. Critical currents were measured when the selected magnetic field. Critical currents were measured when the selected magnetic field is applied first in the increasing direction (labelled as ZFCV data) and then in the decreasing direction (labelled as ZFCD data). In the FC procedure, the sample is allowed to cool from above T_c to the ambient 77 K temperature in a static applied field $B_a = \mu_0 H_a$, then the present field was decreased step by step. Before and after each step the critical currents was measured and the data was labelled as FCD.

3. Results and Discussion

Figure 1 shows the X-ray diffraction patterns of the sample (a) YBCO (b) K-YBCO. It can be seen from the XRD data that the basic structure was single -phase Y(123) and Y(221) phase was in minority. The potassium doping process increased the peak intensity of the peaks (02), (003), (005), (006) (see the inset of Figure 1), whereas it decreased the peak intensity of the peak (103). It was reported [5] that a K_3CuO_2 phase evaporated above 900 °C, which probably occured in our K-YBCO sample.

Typical temperature dependence of resistivity from the sample YBCO and K-YBCO are displayed in Figure 2. The resistive superconducting transition temperature T_c^{onset} is found to be 91 K and 94 K, whereas T_c^{zero} is about 86 and 84 K ($T_{c,\text{midpoint}}$ is 88 and 89.5), hence $\Delta T = T_c^{\text{onset}} - T_c^{\text{zero}} = 5$ and 10 K for pure YBCO and K-doped YBCO, respectively. Therefore K doping of YBCO increased the onset temperature and range of transitions while it deceased the zero resistance temperature. We note that the transition of our YBCO sample occurs at a lower temperature relative to the most of the other data in the literature. However our results correspond to that reported by some other workers (see for example [28] for YBCO bulk and [24] for YBCO film). The transition temperature measured by four probe technique is dependent on the fixed current applied [30]. This was 15 mA for both our YBCO and K-YBCO samples. Observation similar to ours in terms of transition temperature T_c (R=0) [1], T_c^{onset} [5], and critical current density j_c [5] were observed on the samples of K-doped YBCO. Our main purpose was to complement the results of Veneva et al [6]. They displayed the ac susceptibility versus temperature plot of the YBCO samples with $x = 0 - 1.2$ in the batch formula $Y_{1-0.2x}Ba_{2-0.2x}K_xCu_3O_y$, where $x = 0$ and 0.4 correspond to our batch formula of $YBCO$ and $K-YBCO$ samples.

The diamagnetic onset temperature seems to move to a higher temperature similar to the onset resistive transition temperatures of our samples. Our observations show that the transport critical current density decreases, as x increases in contrast with the results reported in Ref. [6]. From Figure 2 it is also noted that the normal state resistivity of K-YBCO is higher than that of pure YBCO.

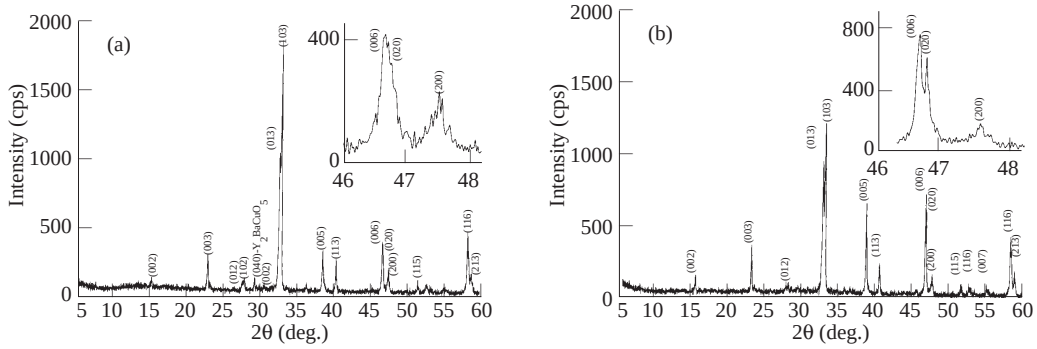

Figure 1. The XRD patterns of (a) YBCO, (b) K-doped YBCO prepared by the conventional solid state reaction method.

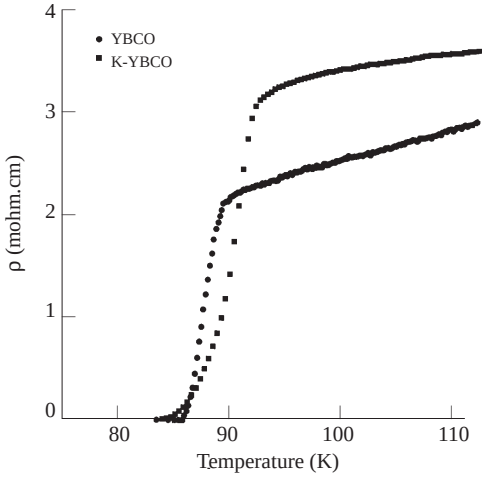

Figure 2. Temperature variation of the resistivity in zero field.

We also explored the resistive transitions in various external magnetic field for both samples. The samples were first zero cooled (ZFC) from above T_c to a chosen temperature below T_c, then the selected static magnet field was applied. Now, while heating, the resistivity versus temperature data was recorded. Figure 3 shows Arrhenius plots of $\ln \rho$ versus T^{-1} for (a) YBCO (b) K-YBCO obtained from the resistive transition data

described above. With increasing applied magnetic field resistive broadening is observed associated with the T_c^{zero} shift to the lower temperature. This well known behavior is attributed to the flux flow resistivity. It is well established that lowering the temperature increases the pinning strength hence the pinning force. When the Lorentz force per unit volume F_L exceeds the pinning force per unit volume F_p, electrical resistance appears because of flux flow. Hence, a higher magnetic field is needed to depin the flux lines at the lower temperature. This results in a shift of the zero-resistance temperature downwards as the magnetic field increases. The slope of these Arrhenius plots in the low resistivity range can be related to the activation energy for thermally activated flux flow or flux creep. In the low current limit, $\rho(B,T) = \rho_0 \exp[-U_0(B,T)/kT]$ [7,8], where $U_0(B,T)$ is the activation energy for the hopping process of a flux line or flux bundle [9,10], and k is the Boltzman constant. From the slopes, we obtained the activation energy values for termally activated flux flow for pure YBCO as 1.034, 0.819, 0.460, 0.498 eV for the field of 0, 25.7, 44.9, 760 mT, respectively. As can be seen in Figure 3b, the low resistivity part of the curve for K-YBCO is much shallower (resulting in much lower activation energy) than that for pure YBCO.

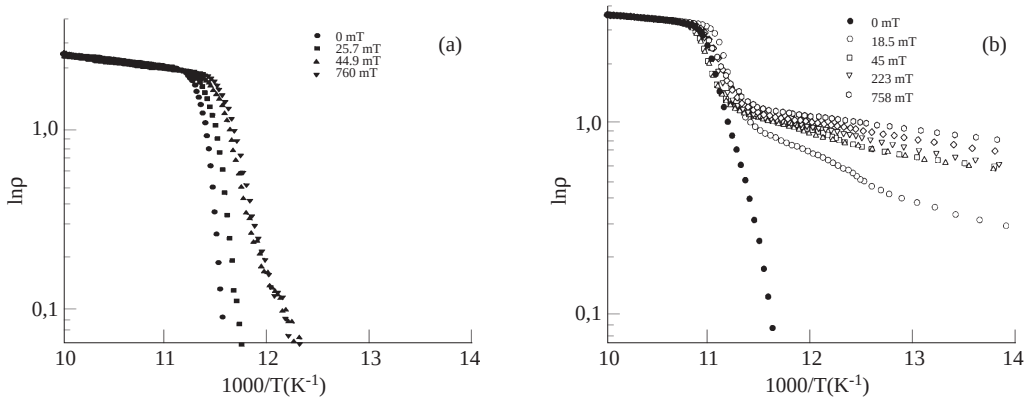

Figure 3. Arrhenius plot of the resistivity in selected magnetic fields for (a) YBCO (b) K-YBCO

In high-T_c superconductors, the critical current, the magnetization and the susceptibility are often dependent on the magnetic history. Evetts and Glowacki [11] observed that critical current of sintered YBCO was hysteretic and attributed this behaviour to the field from trapped flux in the grains. Prior to and since then, an appreciable body of experimental work has been reported on the critical current hysteresis in both Y-Ba-Cu-O (see for example [12-19]) and Bi-Pb -Sr-Ca-Cu-O polycrystalline superconductors [22-24] and Tl-based (1223) superconductors [25]. Several workers [16,24-26] described models (some of them extended EG model) to account for the observed magnetic hysteresis of the critical current in ceramic granular superconductors.

For completenes we also present the critical current hysteresis of our sample. It is well known that the granular nature of these ceramic materials introduces formidable complications in the quantitative analysis of the observations of the various physical properties. Consequently it is desirable to provide additional observations which either support the current and prevailing account or suggest that a new and modified interpretation is needed for the hysteretic behavior of the critical deppinning current I_c.

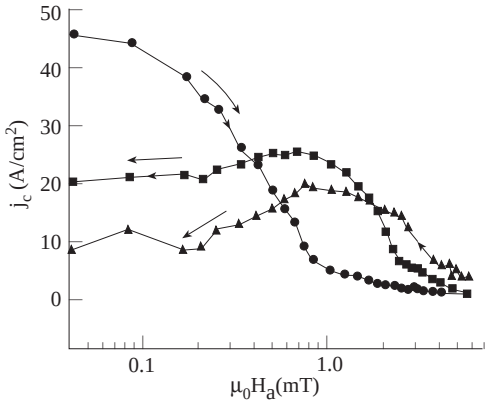

Figure 4. Semilog plot of the transport critical current density for YBCO in increasing and decreasing applied magnetic fields following temperature and field histories described in the text. Solid circles, solid squares and solid triangels represent for ZFCV, ZFCD and FCD data respectively.

The dependence of the critical current density on the history of the magnetic field for the YBCO sample is shown in Figure 4. We note that the critical current behaviour at zero field for the different magnetic histories in agreement with the current account which will be summarized later. The zero field critical current decreases after application of a magnetic field. Figures 6 and 7 displays the current-voltage characteristics of the sample YBCO and K-YBCO sample, respectively, at 77 K in various applied magnetic fields perpendicular to the transport current. The zero field curve for the YBCO shows a notable voltage developing about 2.056 A. As can be seen from Figure 4, j_c for FC procedure at B=6 mT is larger than that for the same field but increased application of the ZFC procedure, i.e. the critical current density at 6 mT of FCD>ZFCV. In the case where the sample is field-cooled and the fields is subsequently decreased to zero (FCD at B=0), the grains are magnetized paramagnetically in which the paramagnetic magnetization is larger than that in ZFCD data at B=0. As a result, $j_c(B = 0)$ for FCD is smaller than that for ZFCD. This quantity also decreases as the maximum excursion field, or the field at which FC procedure was performed, increases. As predicted, the peak of the ZFCD has taken place at the lower applied field than that of the FCD data. The separation of these two peaks depends on the temperature and the critical intragrain current density, dimension and also geometry of the grain [19]. As the temperature

increases, the intragrain critical current density decreases, therefore both peaks move to the lower applied field regions due to the decreases in the paramagnetic moment of the grains. Detailed discussions [12, 16, 19, 25] and experimental results similar to ours can be found in Ref. [12, 19].

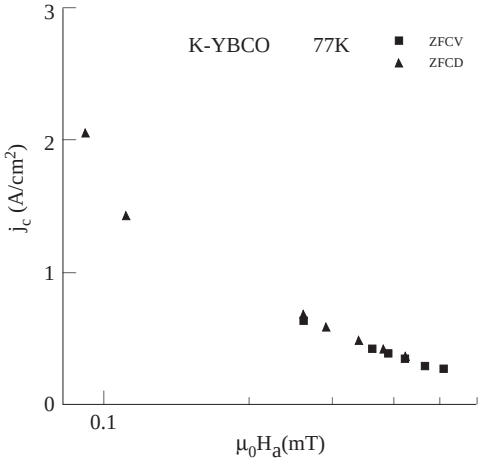

Figure 5. Semilog plot of the transport critical current density for K-YBCO in selected applied magnetic fields for ZFCV and ZFCD histories described in the next.

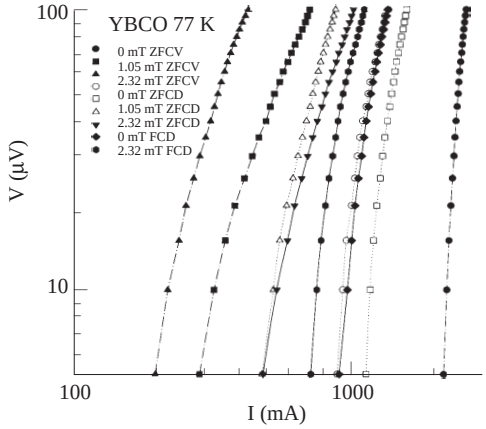

Figure 6. Log-log plot of current voltage characteristics of the YBCO sample at 77 K in selected magnetic fields in increasing (ZFCV), decreasing (ZFCD) and FCD case. ZFCD data was measured after descending from 6 MT.

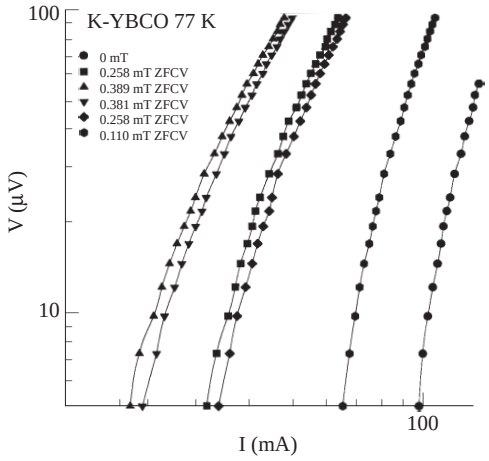

Figure 7. Log-log plot of current voltage characteristics of the K-YBCO sample at 77 K in selected magnetic fields in increasing (ZFCV), decreasing (ZFCD) case.

It is reported in the literature (see for example [11-27]) that the critical conduction current in granular high T_c superconductors depends on the magnetic history of the specimen. This dependence is related with H_g (r), the return field of the magnetized grain. When the applied field H_a has ascended (descended), the return field of the diamagnetically (paramagnetically) magnetized grain is expected to aid (oppose) H_a. Consequently the transport critical current or intergranular current, I_{cm}(r) flows through a larger (smaller) total field, i.e. in the critical state framework, $j_{cm}(r) = \alpha/|H_a \pm H_g(r)|^n$ where α is temperature dependent parameter characterizing the specimen, and n is a constant representing the dependence of the intergrain critical current density j_{cm} on the magnetic flux density, and the positive (negative) sign applies to H_a increasing (decreasing). In the regime where H_a has been decreased from a large value, the individual grains of the sintered granular material become saturated with flux-retaining circulating currents. Thus each grain acquires a magnetic moment μ, hence becomes a small magnet which is magnetized along $\mathbf{H}_a$. Consequently, the critical conduction current is dependent on the magnetic history due to the effect of the magnetization of the grains on the total local field between the grains. If the applied field is smaller than the lower critical field for the grains, H_{c1g}, then a reversible j_c versus H_a curve is expected. Once field penetration into the grains has taken place, reversibility is lost. As can be seen from Figure 5 the K-doped sample shows an almost reversible j_c value (2.3 A/cm^2) at zero applied field. Yang et al. [19] also observed reversible j_c versus H_a curve in pure YBCO for the maximum field smaller than 2 mT. This behavior is attributed to the fact that the maximum applied field is not high enough for penetration into the grains.

4. Summary and Conclusions

We have studied the resistive transition of pure YBCO(123) and K-doped (YBCO

(123) prepared by solid state reaction method in the magnetic field range of 0-760 mT employing the ZFC procedure. The superconducting samples were also characterized by XRD and transport critical current measurements. The activation energy values for TAFF were obtained from the Arrhenius plot of the resistivity vs. temperature. I-V characteristics of the samples in, ZFCV ZFCD and FC procedures at 77 K were measured. With K dopping to YBCO (where $x = 0.4$ in the initial batch formula of $Y_{1-0.2x}Ba_{2-0.2x}K_xCu_3O_y$) we found that : **(i)** the normal state resistivity, the transition temperature T_c^{onset} and transition range ΔT were increased; and **(ii)** the zero resistance temperature $T_c(R=0)$, the activation energy and the critical current density was decreased. For both categories of samples, the activation energy decreases as the applied magnetic field increases. For the YBCO sample the transport critical current hysteresis was observed in the field increasing (ZFCV) and decreasing (ZFCD) direction after an excursion of the field to 6 mT. We conclude that the effect of dopants on the electrical and magnetic properties depends on the heat treatment as well as the initial batch formula which lead the different grain boundary phase structure.

Acknowledgements

We are very grateful to Professor M. A. R. LeBlanc and Professor M. Altunbas for valuable comments and discussions. This work was supported by the Research Fund of Karadeniz Technical University under grant contract no: 97.111.001.01.

References

[1] Y. Saito, T. Noji, A. Endo, N. Higuchi, K. Fugimoto, T. Okawa, and A. Hattori, *Physica,* **148B,** (1987) 336.

[2] Y. Khan, J. Mater. *Sci. Lett.*, **7,** (1988) 53.

[3] R. J. Cava, J. Krajewski, W. Peck, B. Batlogg, Jr. Supp, R. Fleming, and A. James, *Nature*, **338** (1989) 328.

[4] I. Draigeve and I. Nedkov, *IEEE Trans. Magn.* **26,** (1990) 1433.

[5] I. Nedkov and A. Veneva, J. Appl. Phys. **75** (1994) 6726.

[6] A. Veneva, D. K. Petrov, P. Dittrich, and M. J. Naughton, *Physica* **C271,** (1996) 230.

[7] D. Dew-Hughes, *Cryogenics,* **28,** (1988) 674.

[8] T. T. M. Palstra, B. Batlogg, L. F. Schneemeyer, and J. V. Waszczak, *Phys. Rev. Let.* **61,** (1988) 1662.

[9] P. W. Anderson, *Phys. Rev. Lett.,* **9**, (1962) 309.

[10] P. W. Anderson and Y. B. Kim, *Rev. Mod. Phys.,* **36,** (1964) 39.

[11] J. E. Evetts and B. A. Glowacki, *Cryogenics* **28,** (1988) 641.

[12] M. E. McHenry, M. P. Maley and J. O. Willis, *Phys, Rev.,* **B 40** (1989) 2666.

[13] J. O. Willis, M. E. McHenry, M. P. Maley, and H. Sheinberg, *IEEE Trans. Magn.,* **25,** (1989) 2502.

[14] R. Jones, R. A. Doyle, F. J. Blunt and A. M. Campbell, *Physica* **C 196,** (1992) 63.

[15] K. H. Muller and D. N. Matthews, *Applied Supercon. Conf., Chicago,* August 24, 1992.

[16] E. Altshuler, J. Barroso, A. R. R. Papa and V. Venegas, *Cryogenisc* **33,** (1993) 308.

[17] U. Dai, G. Deutscher, C. Lacour, F. Laher-Lacour, P. Mocaer and M. Lagues, *Appl. Phys. Lett.,* **56,** (1990) 1284.

[18] K. Tsukamoto, M. Ishii, H. Shimojima, C. Yamagishi, M. Takata and T. Yamashiat, *Jpn. J. Appl. Phys.,* **31,** (1992) L464.

[19] Y. Yang, C. Beduz and S. P. Ashworth, *Cryogenics,* **30,** (1990) 619.

[20] F. Grivon, J. Bouthegourd, A. Leriche and P. Macaër, *Physica* **C 235**, (1994) 3447.

[21] M. majoros, M. Polak, V. Strbik, S. Benacka, S. Chromik, F. Hanic and V. Plechacek, *Supercond. Sci. Technol.,* **3,** (1990) 227.

[22] P. Muné, E. Altshuler, J. Musa, and S. Garcia, *Physica* **C 226,** (1994) 12.

[23] P. Muné and J. López, *Physica* **C 257**, (1996) 360.

[24] P. Muné and J. López, *Physica* **C 261**, (1996) 173.

[25] F. A. List, D. M. Kroeger, and V. Selvamanickam, *Physica* **C 275**, (1997) 220.

[26] K. H. Müller and D. N. Matthews, *Physica* **C 206,** (1993) 275.

[27] S. Çelebi and M. A. R. LeBlanc, *Phys. Rev.,* **B49**, (1994) 16009.

[28] M. Nikolo, L. M. Stacey and M. J. Missey, *Physsica* **B194-196,** (1994) 1875.

[29] V. Pagnon, C. Villard, C. Ayache and J. C. Villgier, *Physica* **B 169,** (1991) 645.

[30] H. Niu, N. Fukushima and K. Endo, *Japanese Journal of Appl. Phys.,* **27,** (1988) L1442.